

Rapid Study on Feature Extraction and Classification Models in Healthcare Applications

S. Sowmyayani

Abstract—The advancement of computer-aided design helps the medical force and security force. Some applications include biometric recognition, elderly fall detection, face recognition, cancer recognition, tumor recognition, etc. This paper deals with different machine learning algorithms that are more generically used for any health care system. The most focused problems are classification and regression. With the rise of big data, machine learning has become particularly important for solving problems. Machine learning uses two types of techniques: supervised learning and unsupervised learning. The former trains a model on known input and output data and predicts future outputs. Classification and regression are supervised learning techniques. Unsupervised learning finds hidden patterns in input data. Clustering is one such unsupervised learning technique. The above-mentioned models are discussed briefly in this paper.

Keywords—Supervised learning, unsupervised learning, regression, neural network.

I. INTRODUCTION TO CLASSIFICATION SYSTEM

THE recent advancements in computing, machine learning, and image recognition have a significant impact on the automatic detection of various diseases. Several screening approaches are now used to detect suspicious diseases. Computer-Aided Diagnosis (CAD) is able to assist doctors in understanding medical images, allowing for cancer diagnosis with greater accuracy, which is critical for patients. It has been demonstrated that Deep Convolutional Neural Networks (DCNN) are effective at image classification, object detection and other visual tasks. They have had a lot of success with applications for medical imaging.

The sciences of biology and medicine have greatly benefited from computational methods. These methods aid medical professionals in early anomaly diagnosis and successful therapy. This paper discusses various health care applications that can be solved using CAD. The architecture of all those applications follows the same procedure.

A. Conventional Architecture

The traditional architecture of any classification system follows the same procedure. Supervised learning trains the dataset before testing. Hence, the dataset is divided into training and testing sets. In both training and testing, there are four important phases. They are preprocessing, segmentation, feature extraction, and classification. This section briefly discusses all these phases. Machine learning feature extraction

and classification are elaborated in [1]. Fig. 1 shows the conventional architecture of the classification model.

Data Splitting

The dataset is split into training and testing tests. The splitting is done in a random ratio. Most of the classification systems follow an 80:20 ratio for training and testing. Other ratios are 90:10, 70:30, 60:40, and 50:50. The larger the training dataset, the more accurate the classification will be. But a good classification system should give accurate results even with less training.

Pre-Processing

Pre-processing is first carried out to enhance the caliber of image visualization. Each digital image should be evaluated for its common components, such as noise, background, brightness, blur, intensity changes, etc., after being taken and before algorithm applications are launched. Pre-processing is an excellent way to complete this activity. The performance of the classification system is enhanced by this step.

Segmentation

The process of segmenting an image into objects or groups is called segmentation. The affected area in medical images should be subdivided to determine whether a disease is severely affecting a patient. The four main types of image segmentation are clustering-based segmentation, region-based segmentation, edge-based segmentation and mask R-CNN.

Region-Based Segmentation

In region-based segmentation, the regions into which the objects are divided are determined by a threshold value(s). Both a global and local threshold could exist. This strategy works particularly well when there is a lot of contrast between the object and the background. The main disadvantage is that it becomes extremely challenging to obtain precise segments when there is no discernible grayscale difference or an overlap of the grayscale pixel values.

Edge-Based Segmentation

This technique employs discontinuous local aspects of an image to identify edges and subsequently determine the object's border. Images benefit from having stronger object contrast. When there are too many edges in the image or when there is less contrast between objects, edge-based segmentation is not appropriate.

S. Sowmyayani is with Department of Computer Science, St. Mary's College (Autonomous), Thoothukudi, Tamilnadu, India (e-mail: sowmyayani@gmail.com)

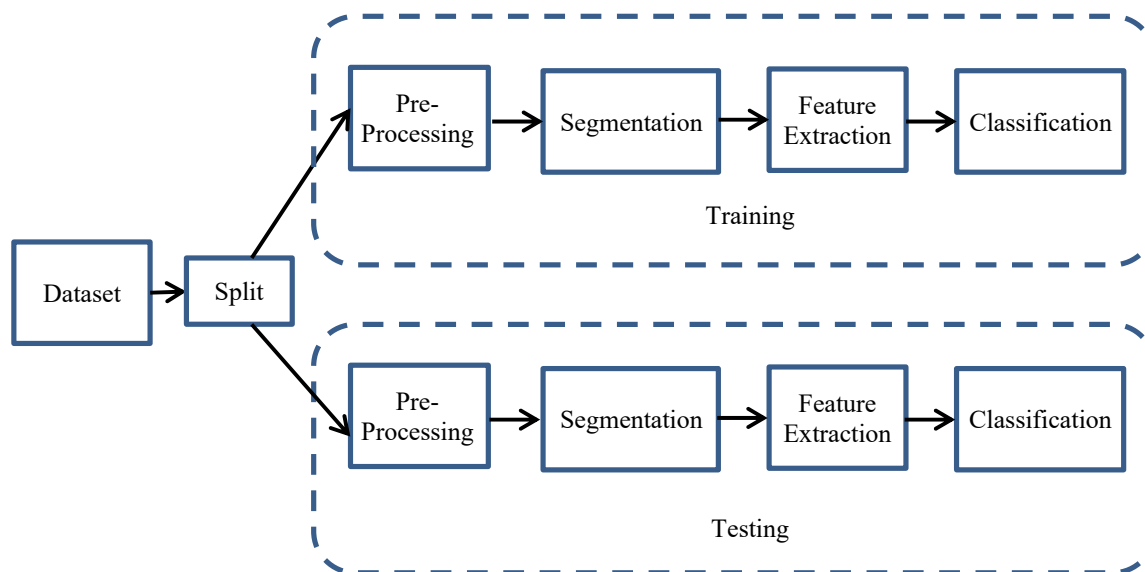


Fig. 1 Conventional Architecture of Classification Model

Clustering-Based Segmentation

With this technique, the image's pixels are separated into homogeneous clusters. It produces nice clusters and performs exceptionally well on tiny datasets. The main disadvantage is the very long and expensive computation time. One approach that is unsuitable for grouping non-convex clusters is K-means.

Mask R-CNN

Each item in the image receives three outputs from this method: the class, bounding box coordinates, and object mask. It is easy to use and adaptable. Additionally, it represents the state-of-the-art in image segmentation. The approach has a long training period.

Feature Extraction

The technique of turning raw data into useful features that can be handled easily in the further processing is known as feature extraction. It improves the performance of the method rather using the raw data directly.

Feature extraction can be accomplished manually or automatically:

- Manual feature extraction includes defining the characteristics that are pertinent to a particular issue and putting in place a method to extract those features. Having a solid grasp of the context or domain can often aid in making decisions about which characteristics might be helpful. Engineers and scientists have created feature extraction techniques for images, signals and text through many years of research.
- Without requiring human input, automated feature extraction uses specialized algorithms or deep networks to automatically extract features from signals or images. When you need to go from collecting raw data to creating machine learning algorithms quickly, this method can be quite helpful.

The first layers of deep networks have largely taken the

position of feature extraction with the rise of deep learning, albeit mostly for image data. Prior to developing powerful prediction models for signal and time-series applications, feature extraction continues to be the first hurdle that demands a high level of knowledge.

A vector containing a list of features is created by the feature extraction algorithm. This creates a reliable representation of the item and is known as a "feature vector," which is a 1D array. It is crucial to note that the 1D array only represents one feature. The ability to repeat a feature is a crucial quality. The feature should actually be able to recognize items in general, not just this one in particular. As a result, in real-world problems, the feature will not be a perfect replica of the component in the input image. This feature will not be duplicated in another object. Rather, it appears to have features that are comparable to every feature in the training dataset. When the feature extractor encounters a large number of related items, regardless of where they appear in the image or what kind of object they are, it detects patterns that define the object in general.

Classification

Image classification is a complicated process that depends on various factors. This phase classifies the features into classes. There have been several classifier models introduced so far [2].

II. HEALTHCARE APPLICATIONS

Here are some important healthcare applications that can be diagnosed if they are treated earlier. The machine helps to identify the disease quickly and earlier than human identifies.

A. Brain Tumor Detection

The primary method for early tumor diagnosis and treatment planning is brain tumor segmentation. Although there are a number of brain tumor segmentation methods, effective tumor segmentation methods are still difficult to

utilize because brain tumor images have complex properties. Along with tumor heterogeneity, tumor borders can also be complicated and ill-defined aesthetically. Doctors analyze brain tumors, but depending on the doctor's level of skill, their grading results in varied conclusions.

A diverse range of central nervous system neoplasms that develop inside or around the brain is called brain tumors [3]. Additionally, the symptoms of the patient, surgical treatment alternatives, and the possibility of receiving a conclusive diagnosis are all significantly impacted by the tumor's location within the brain. The risk of neurological toxicities that affect the patient's quality of life is also significantly altered by the tumor's location. Currently, imaging is only used to find brain tumors after the beginning of neurological symptoms. Even in people who are known to be predisposed to certain types of brain tumors due to their genetic makeup, no current early detection methods are available.

The World Health Organization (WHO) modified the current histopathological classification systems in 1999 [4]. These classifications, which are based on the assumed cell of origin of tumors, have been in use for nearly a century. Although they are satisfactory in many ways, neither provides the precise guidance that patients and doctors would need or expect when making therapeutic decisions about a given patient's tumor activity. The main methods for proving that neurological symptoms are brought on by a brain tumor are current imaging techniques, which provide thorough anatomical delineation.

A medical procedure known as Magnetic Resonance Imaging (MRI) allows radiologists to see into the human body without having to perform surgery. MRI offers a wealth of knowledge about human soft tissue, which aids in the identification of brain cancers. For computer-aided clinical tools to accurately diagnose brain cancers, MRI images must be segmented accurately [4]. Tumors are categorized as malignant or benign after proper segmentation of brain MR images, which is a challenging task due to the complexity and variety of tumor tissue characteristics such as shape, size, gray level intensities and location.

B. Diabetic Retinopathy

Prior to the patient experiencing more severe symptoms, Diabetic Retinopathy (DR) can damage the retina's blood vessels. The damage to the retina is not uniformly distributed, so a patient with DR will have a different relationship between their pupil's response to a light stimulus on the retina's center and on its periphery than a healthy individual would. Retinal pictures, or images of the ocular fundus, can help in the diagnosis and treatment of ophthalmic, retinal, and even systemic disorders like diabetes, hypertension, and arteriosclerosis. Early diagnosis and screening of DR can be aided by automatic lesion detection in retinal pictures. Exudates are the DR's main symptom. Therefore, the primary prerequisite for diagnosing the development of DR is the identification of exudates.

It might be difficult to identify DR early because patients will not have any symptoms until visual loss starts to happen.

DR is a degenerative condition that progresses from Non-Proliferative Diabetic Retinopathy (NPDR) to Proliferative Diabetic Retinopathy (PDR). The initial stage of DR is known as NPDR, while the most advanced stage is known as PDR. This can be found during the annual screening process for diabetic individuals looking for any indication of NPDR. Fundus photography has been proven to be the most reliable method of retinopathy screening. In the majority of developing nations, there are not enough experts in remote areas to conduct ophthalmologists' examinations of diabetic patients as part of screening programs.

NPDR is an early indicator of DR and is often referred to as background retinopathy. The mild NPDR that precedes the DR typically has little impact on vision. Exudates (EXs), a condition in which proteins such as lipoproteins or other substances seep from blood vessels in the retina, impair vision. EXs come in two different types: hard EXs (yellow dots seen in the retina) and soft EXs (pale yellow or white areas with ill-defined edges).

C. Glaucoma Detection

A condition known as glaucoma affects the eyes by raising intraocular pressure, which in turn damages the optic nerve. This condition is brought on by the release of too much fluid into the eye. Permanently harming the retina and the optic nerve can reduce eyesight. If it is not discovered sooner, it will result in blindness. Since it commonly advances without showing any signs, glaucoma is a severe eye disorder that causes vision loss. Finding early glaucoma requires a suspicious infection of the optic nerve and is challenging. In comparison to digital fundus images, the diagnosis of glaucoma using Optical Coherence Tomography (OCT) and Heidelberg Retinal Tomography (HRT) is relatively expensive [5], [6]. It is simple to identify glaucoma-suspicious characteristics in fundus images, such as the optic disc and cup [7]-[9].

The two types of glaucoma detection are primary open angle glaucoma and secondary glaucoma. When glaucoma is discovered at a relatively young age, the condition is known as primary open angle glaucoma. It is secondary glaucoma if it is discovered later on. A stereo optic disc image is used by an Optic Nerve Head (ONH) to detect structural abnormalities in glaucoma. Stereo images are used to create the stereo optic disk images, which create the illusion of cup depth. This depth is a crucial glaucoma warning sign.

Monocular stereo optical images have been extensively studied. By generating the ONH depth map using stereo-matching techniques, these images are used to ascertain the alterations in the optic nerve [10], [11]. The Cup-to-Disc Ratio (CDR), a metric that is frequently used to detect elongation of the optic cup and loss of the neuro-retinal rim, is calculated from the optic disc and cup.

D. Mammogram Abnormalities

One of the most common malignancies in women is breast cancer, and it has one of the highest fatality rates [12]. Early cancer detection has the potential to save human lives.

Because mammography takes an image of the breast tissue, it is a great help to medical science. The doctor can identify breast cancer early thanks to this help. Consequently, mammography serves as a screening technique for finding breast cancer. The cluster of calcifications is the first sign of breast cancer.

In the breast tissue, microcalcification typically refers to a minute calcium deposit. The morphology of this calcium deposit can be round, lobular, specular, or asymmetrical. These microcalcifications appear as tiny granules on a mammogram, and it is quite challenging for the doctor to precisely pinpoint where they are. One study found that between 10% and 40% of microcalcifications are ignored by clinicians [13]. However, if the system is properly educated, computers can easily detect irregularities. An efficient CAD system can assist doctors in earlier cancer detection by utilizing cutting-edge image processing techniques [14]. The segmented mammography image in [15] is identified using an Extreme Learning Machine (ELM) classifier, and three distinct features are derived from it.

In the literature, a number of CAD systems have already been reported [13]-[15]. The majority of the current systems have high false positive and false negative rates. As a result, there is always a need for a CAD system to detect breast cancer.

E. Fall Detection

The occurrence and detection of falls in the elderly are increasing. This requires researchers and healthcare professionals to create an efficient method in order to detect and prevent these uncertain situations. The WHO stated that the effects of falls are growing worldwide [16]. From their report, it is clear that around 28-35% of people of age 65 fall every year, and within that, 32-42% of people are of age 70. The fall rate increases as the number of elderly people increases. More than one of every five people in a group will likely be 65 or older by 2050, on average. This is likely to encourage a higher fall rate.

In order to prevent elderly falls, fall detection systems must be developed. A keyframe-based fall detection system for aged care systems is introduced in 2021 [17]. Following this, an effective fall detection approach using correlation and motion history images is developed [18]. The environment, a person's conduct and a person's characteristics all have a role in the causes of falls. Assistance is required to prevent the emergence of these variables.

F. Lung Cancer Detection

According to WHO statistics, cancer was the major cause of 8.8 million deaths worldwide in 2015 [19]. Lung cancer accounted for 1.69 million, or close to 20%, of all deaths. Because cancer is most effectively treated when discovered in its early stages, cancer screening is crucial to preventative healthcare. Malignant lung nodules frequently have lobulations, spiculated contours and inhomogeneous attenuation in their appearances. Currently, lung cancer screening with Low Dose Computed Tomography (LDCT) is

quite significant.

For those in high-risk groups, LDCT screening is advised because it has decreased lung cancer fatalities. Standard dosage Computed Tomography (CT) may be used to further analyze the outcomes of LDCT screening. The implementation of LDCT screening is hampered by a number of issues, including providers' concerns about access to the necessary equipment and potential cost constraints on rural populations. Rural people also have limited access to specialists and primary care doctors. On the other hand, rural communities have easy access to chest x-rays. However, compared to LDCT or CT scans, chest x-rays provide images of inferior resolution; as a result, a lower quality diagnosis is typically anticipated.

G. Skin Cancer Detection

One of the most difficult problems facing modern medicine is cancer [20]-[22]. It starts when cells in a certain area of the body expand wildly and uncontrollably. The nutrients from the healthy, strong cells are taken up by these cancer cells. As a result, the body becomes weaker and the immune system is no longer able to defend the body against diseases. These cancer cells may spread to other regions of the body from the affected part. The liver, lung, bone, breast, prostate, bladder, and rectum are just a few of the body parts that can be impacted by cancer. The skin is another area that can be affected.

Melanoma and non-melanoma skin cancers can be divided into two categories [23], [24]. In 2017, there were 132,000 cases of melanoma and between two and three million cases of non-melanoma skin cancer worldwide, according to WHO estimates [24]. The fastest-growing form of skin cancer and the one that results in the most fatalities is melanoma. In general, radiation therapy, chemotherapy, immunotherapy, etc., or their combinations, can cure all types of skin cancer. However, the effectiveness of the treatment plan depends on how quickly patients are identified and treated.

The ABCD rule (Asymmetry, Border, Colour, Diameter) [25] is used to identify melanoma skin cancer. Color channel optimization [26]-[28], level set-based techniques [29], [30], iterative stochastic regions merging [31], deep learning with convolution neural networks [32]-[37] and other techniques are used to segment skin lesions. On the one hand, level set methods and segmentation techniques based on color channel optimization are typically not very accurate. Additionally, the results are influenced by various elements such as hairs and signs that have been marked with pens or rules, and these approaches are unable to accurately partition very low-density zones, among other things. On the other hand, modern deep learning-based techniques need a lot of training data and a lot of time and resources for computation. Furthermore, in order to generate final segmentations with high accuracy in supervised deep learning models, large-scale training data including the numerous parameters stated above is essential.

III. RESULTS DISCUSSION

A. Segmentation Results

This section discusses some of the graphical results obtained in health care applications discussed in the previous section. Fig. 2 shows the optic disc and cup segmentation of glaucoma detection results.

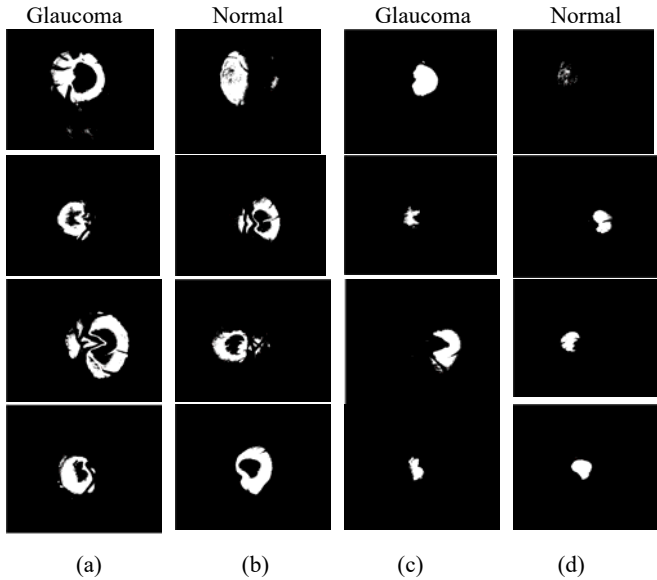


Fig. 2 (a) and (b) Optic disc segmentation; (c) and (d) Optic cup segmentation

It is observed that the size of the glaucoma affected cup is larger than the normal eyes. Fig. 3 shows the affected regions in mammogram images. The malignant and benign tumor regions are segmented in Fig. 4.

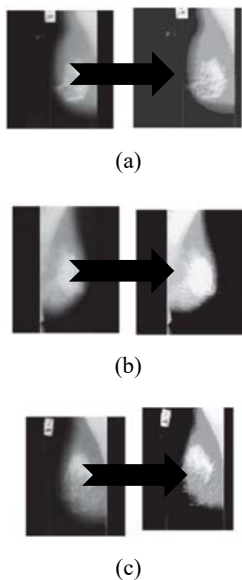


Fig. 3 Input and its Segmented Image: (a) Normal (b) Benign (c) Malignant Mammograms

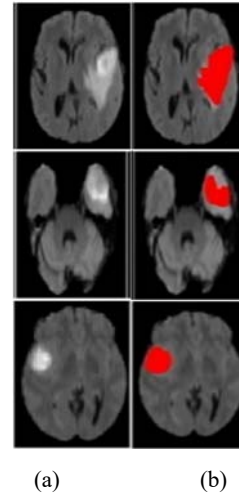


Fig. 4 Tumor Segmentation in MRI Images: (a) Original Image and (b) Segmented Image

Fig. 5 shows the hard EXs detection in eye images. Lungs and its segmented images are shown in Fig. 6. The skin cancer segmentation results are shown in Fig. 7.

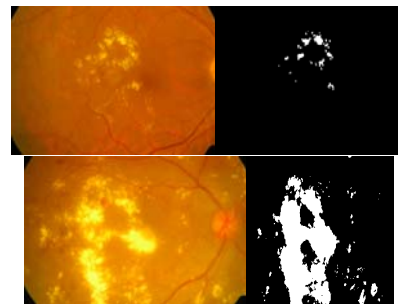


Fig. 5 Fundus images and the detection of hard EXs results



Fig. 6 Original Lung and its Segmented Image

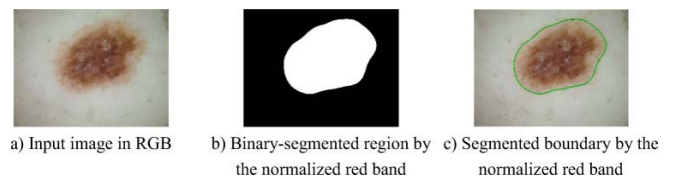


Fig. 7 Skin Cancer Segmentation Results

A. Performance Measures

To analyze the performance of the segmentation methods, accuracy, Positive Predictive Value (PPV), Dice Similarity Coefficient (DSC), Jaccard Index (JI), Sensitivity and Specificity are used. Table I displays the formula for all the

metrics.

TABLE I
FORMULA FOR THE METRICS

| Measure | Formula |
|-------------|---|
| Accuracy | $Ac_r = \frac{TP+TN}{TP+TN+FP+FN} \times 100$ |
| PPV | $PPV = \frac{TP}{TP+FP}$ |
| Sensitivity | $Sensitivity = \frac{TP}{TP+FN}$ |
| Specificity | $Specificity = \frac{TN}{FP+TN}$ |
| DSC | $DSC = \frac{2 \times TP}{FP+(2 \times TP)+FN}$ |
| JI | $JI = \frac{TP}{TP+FP+FN}$ |

B. Common Datasets

This section discusses some of the common datasets used in each healthcare application. Most of the mentioned datasets are publicly available. Table II summarizes the common dataset of the discussed healthcare applications.

TABLE II
COMMON DATASETS

| Application | Common Datasets |
|-------------------------|--|
| Brain Tumor Detection | BRATS 2012, 2013, 2014, 2015, 2016, 2017, 2018, 2019, 2020 [38] |
| Glaucoma Detection | RIM-ONE [39], ACRIMA [40], ORIGA [41], HRF [42], Drishti-GS1 [43], sjchoi86-HRF [44] |
| DR | IDRiD [45], DRIVE [46], Messidor-2 [47] |
| Mammogram Abnormalities | MIAS [48], DDSM [49] |
| Fall Detection | Video-based Datasets: UP Fall [50], MobiFall [51], |
| Lung Cancer | JSRT [52], ChestX-ray14 [53, 54] |
| Skin Cancer | ISIC [55] |

Table III displays the common datasets used in brain tumor segmentation.

TABLE III
COMMON DATASETS IN BRAIN TUMOR DETECTION

| Dataset | Description | Accuracy (%) |
|------------|--|--------------|
| BRATS 2012 | 3875 training, 3875 testing | 100 [56] |
| BRATS 2013 | 4650 training, 1550 testing | 92.2 [56] |
| BRATS 2014 | 3000 training, 15500 testing | 98.5 [56] |
| BRATS 2015 | Size 240 x 240 x 155 32,020 training and 24,180 testing | 99.09 [57] |
| BRATS 2016 | 19032 non-glioma 15272 glioma | 99.45 [57] |
| BRATS 2017 | 210 images | 99.54 [57] |
| BRATS 2018 | 29605 training, 10320 testing | 92.67 [58] |

TABLE IV
COMMON DATASETS IN GLAUCOMA DETECTION

| Dataset | Description | Results |
|--------------|---|---|
| RIM-ONE | Size 2144x 1424 85 are normal eyes, and 74 are glaucomatous eyes | 96.1% DSC for disc and 84.45% DSC for cup [59] |
| ACRIMA | 396 glaucoma and 309 non-glaucoma Size between 1944x2108 and | 0.77 AUC [60] |
| ORIGA | 2426x3007 pixels. 296 glaucoma and 724 non-glaucoma | 0.85 AUC [61] |
| HRF | 27 glaucoma and 18 non-glaucoma | 0.95 AUC [60] |
| Drishti-GS1 | 2896 x 1944 70 glaucoma and 31 non-glaucoma | 97.38% DSC for Disc and 88.77% DSC for cup [59] |
| sjchoi86-HRF | 101 glaucoma and 300 non-glaucoma | 0.85 AUC [60] |

TABLE V
COMMON DATASETS IN DR

| Dataset | Description | Results |
|------------|--------------------------|---------------------|
| IDRiD | 516 images | 0.95 AUC [62] |
| DRIVE | 33 normal and 7 abnormal | 97.5% Accuracy [63] |
| Messidor-2 | 1748 images | 0.95 AUC [62] |

Tables IV and V give the common datasets and recent results obtained in Glaucoma detection and DR methods respectively.

In Tables IV and V, AUC denotes Area Under ROC Curve. ROC is a Receiver Operating Characteristics which is plot between true positive rate and false positive rate. Tables VI and VII show the datasets and the results obtained by mammogram abnormalities detection and fall detection methods respectively.

TABLE VI
COMMON DATASETS IN MAMMOGRAM ABNORMALITIES

| Dataset | Description | Results |
|---------|---|---------------------|
| MIAS | 322 images of size 1024 x 1024, 204 normal 118 abnormal | Accuracy 98.2% [64] |
| DDSM | 5282 training, 278 testing | 0.85 AUC [65] |

TABLE VII
COMMON DATASETS IN FALL DETECTION

| Dataset | Description | Accuracy (%) |
|----------|-------------|--------------|
| UP Fall | 17 subjects | 95.1 [66] |
| MobiFall | 24 subjects | 99.12 [66] |

In Tables VI and VII, the accuracy is higher than 95%. It shows the performance of the good classification models. Tables VIII and IX show the common datasets and the results obtained by lung cancer and skin cancer detection methods respectively.

TABLE VIII
COMMON DATASETS IN LUNG CANCER

| Dataset | Description | Results |
|--------------|---------------------------------------|---------------|
| JSRT | 247 images 154 abnormal, 93 normal | 97.5 DSC [67] |
| ChestX-ray14 | 112120 images | 0.94AUC [68] |

TABLE IX
COMMON DATASETS IN SKIN CANCER

| Dataset | Description | Results |
|---------|--------------|--------------|
| ISIC | 23000 images | 95% AUC [69] |

IV. CONCLUSION

Researches are developing in the field of medicine over past few decades. This paper discusses some common health care applications. It also elaborates each phase in segmentation and classification models. An overview is given to the common datasets and the performance metrics used to evaluate the classification models. This paper helps the junior researchers in developing the best classification model for health care applications. It also guides to get the datasets for various applications.

REFERENCES

- [1] Sowmyayani. S, 2022, Machine Learning. In Kumar, A., Sagar, S.,

- Kumar, T.G. and Kumar, K.S. eds., 2022. *Prediction and Analysis for Knowledge Representation and Machine Learning*. CRC Press.
- [2] Sowmyayani, S., 2022. A Handbook on Healthcare Applications. A Handbook on Healthcare Applications, BPI Publications, ISBN: 978-93-5547-948-8, pp.1-42.
- [3] D. N. Louis et al., "The 2007 WHO classification of tumours of the central nervous system," *Acta Neuropathologica*, vol. 114, no. 2, pp. 97–109, 2007.
- [4] Kleihues, P., Louis, D.N., Scheithauer, B.W., Rorke, L.B., Reifenberger, G., Burger, P.C. and Cavenee, W.K., 2002. The WHO classification of tumors of the nervous system. *Journal of Neuro pathology & Experimental Neurology*, 61(3), pp.215-225.
- [5] U.R., Chau, K. C., Ng, E. Y. K., Wei, W., and Chee, C., "Application of higher order spectra for the identification of diabetes retinopathy stages". *J. Med Syst.*
- [6] Song, X., Chen, Y., Song, K., and Chen, Y., "A Computer – based diagnosis of glaucoma using an artificial neural network". Proceedings of 17th Annual Conference IEEE Engineering in Medicine and Biology, 1, 847-848, 1995.
- [7] Viranee Thongnuch, Bunyarit Uyyanonvara, "Automatic optic disc detection from low contrast retinal images of ROP infant using mathematical morphology", 2000.
- [8] Nayak, J. Bhat, P.S., Acharya, U. R., Lim, C.M., and Kagathi, M., "Automated identification of different stages of diabetic retinopathy using digital fundus images". *J. Med. Sys.*, 2008.
- [9] L. Tang, et al., "Robust Multiscale Stereo Matching from Fundus Images with Radiometric Differences," *IEEE Transactions on Pattern Analysis and Machine Intelligence*, vol. 33, no. 11, pp. 2245–2258, Nov. 2011.
- [10] T. Nakagawa, et al., "Quantitative depth analysis of optic nerve head using stereo retinal fundus image pair," *J. Biomed. Opt.*, vol. 13, no. 6, pp. 064026–064026–10, 2008.
- [11] URL: <http://www.who.int/whosis/mort/en/index.html>, 2006.
- [12] R.G. Bird, T.W. Wallace, B.C. Yankaskas, "Analysis of cancers missed at screening mammography," *Radiology*, vol. 184, pp. 613–617, 1992
- [13] H. Burhenne, L. Burhenne, F. Goldberg, T. Hislop, A.J. Worth, P.M. Rebbeck, and L. Kan, "Interval breast cancers in the screening mammography program of British Columbia: Analysis and classification," *Am. J Roentgenol.*, vol. 162, pp.1067–1071, 1994
- [14] Lee SK, Lo CS, Wang CM, Chung PC, Chang CI, Yang CW, Hsu PC: A computer-aided design mammography screening system for detection and classification of microcalcifications. *Int J Med Inform* 60(1):29–57, 2000
- [15] Sowmyayani, S. and Murugan, V., 2021. Multi-Type Classification Comparison of Mammogram Abnormalities. *International Journal of Image and Graphics*, 21(03), p.2150027.
- [16] World Health Organization, World Health Organization. Ageing and Life Course Unit, 2008. WHO global report on falls prevention in older age. World Health Organization.
- [17] Sowmyayani, S., Murugan, V. and Kavitha, J., 2021. Fall detection in elderly care system based on group of pictures. *Vietnam Journal of Computer Science*, 8(02), pp.199-214.
- [18] Sowmyayani, S. and Rani, P.A.J., 2019. An efficient fall detection method for elderly care system. *International Journal of Computer and Information Engineering*, 13(3), pp.173-177.
- [19] World Health Organization, 2015. Global health observatory data repository. 2011. Number of deaths (World) by cause.
- [20] "Melanoma: Statistics," American Cancer Society, Jul. 2016. (Online). Available: <https://www.cancer.net/cancer-types/melanoma/statistics>. Accessed 6 Nov. 2018
- [21] "Melanoma skin cancer," European Commission, 2017. (Online). Available: https://ec.europa.eu/research/health/pdf/factsheets/melanoma_skin_cancer.pdf. Accessed 6 Nov. 2018
- [22] Seyed HH, Mohammadamin D. Review of cancer from perspective of molecular. *Journal of Cancer Research and Practice*. 2017;4(4):127–129.
- [23] Yu Lequan, Chen Hao, Dou Qi, Qin Jing, Heng Pheng-Ann. Automated Melanoma Recognition in Dermoscopy Images via Very Deep Residual Networks. *IEEE Transactions on Medical Imaging*. 2017; 36(4): 994–1004. doi: 10.1109/TMI.2016.2642839.
- [24] Esteva A, Kuprel B, Novoa RA, Ko J, Swetter SM, Blau HM, Thrun S. Dermatologist-level classification of skin cancer with deep neural networks. *Nature*. 2017; 542:115–118. doi: 10.1038/nature21056.
- [25] M. Kunz and W. Stolz, "ABCD rule," *Dermoscopia Organization*, 17 Jan. 2018. (Online). Available: https://dermoscopia.org/ABCD_rule. Accessed 11 Nov. 2018
- [26] A. A. A. Al-abayechi, X. Guo, W. H. Tan and H. A. Jalab, "Automatic skin lesion segmentation with optimal colour channel from dermoscopic images," *ScienceAsia*, vol. 40S, pp. 1–7, 2014.
- [27] D. N. H. Thanh, U. Erkan, V. B. S. Prasath, V. Kumar and N. N. Hien, "A Skin Lesion Segmentation Method for Dermoscopic Images Based on Adaptive Thresholding with Normalization of Color Models," in *IEEE 2019 6th International Conference on Electrical and Electronics Engineering*, Istanbul, 2019.
- [28] D. N. H. Thanh, N. N. Hien, V. B. S. Prasath, U. Erkan, K. Adytia: Adaptive Thresholding Skin Lesion Segmentation with Gabor Filters and Principal Component Analysis," in *The 4th International Conference on Research in Intelligent and Computing in Engineering RICE'19*, Hanoi, 2019
- [29] D. N. H. Thanh, N. N. Hien, V. B. S. Prasath, L. T. Thanh and N. H. Hai, "Automatic Initial Boundary Generation Methods Based on Edge Detectors for the Level Set Function of the Chan-Vese Segmentation Model and Applications in Biomedical Image Processing," in *The 7th International Conference on Frontiers of Intelligent Computing: Theory and Application (FICTA-2018)*, Danang, 2018.
- [30] Z. Ma and J. M. R. S. Tavares, "Segmentation of Skin Lesions Using Level Set Method," in *Computational Modeling of Objects Presented in Images. Fundamentals, Methods, and Applications (Lecture Notes in Computer Science, vol 8641)*, Springer, 2014, pp. 228–233.
- [31] Wong A., Scharcanski J., Fieguth P. Automatic Skin Lesion Segmentation via Iterative Stochastic Region Merging. *IEEE Transactions on Information Technology in Biomedicine*. 2011;15(6):929–936. doi: 10.1109/TITB.2011.2157829.
- [32] Al-Masni MA, Al-Antari MA, Choi MT, Han SM, Kim TS. Skin lesion segmentation in dermoscopy images via deep full resolution convolutional networks. *Computer Methods and Programs in Biomedicine*. 2018;162:221–231. doi: 10.1016/j.cmpb.2018.05.027.
- [33] M. Berseth, "ISIC 2017-Skin Lesion Analysis Towards Melanoma," *arXiv:1703.00523*, 2017.
- [34] Y. Yuan, "Automatic skin lesion segmentation with fully convolutional-deconvolutional networks," *arXiv:1703.05165*, 2017.
- [35] L. Bi, J. Kim, E. Ahn, D. Feng and M. Fulham, "Semi-automatic skin lesion segmentation via fully convolutional networks," in *2017 IEEE 14th International Symposium on Biomedical Imaging (ISBI 2017)*, Melbourne, 2017.
- [36] Jaisakthi SM, Mirunalini P, Aravindan C. Automated skin lesion segmentation of dermoscopic images using GrabCut and k-means algorithms. *IET Computer Vision*. 2018;12(8):1088–1095.
- [37] Burdick J, Marques O, Weinthal J, Furht B. Rethinking Skin Lesion Segmentation in a Convolutional Classifier. *Journal of Digital Imaging*. 2018;31(4):435–440.
- [38] H. Menze, A. Jakab, S. Bauer, J. Kalpathy-Cramer, K. Farahani, J. Kirby, et al. "The Multimodal Brain Tumor Image Segmentation Benchmark (BRATS)", *IEEE Transactions on Medical Imaging* 34(10), 1993-2024 (2015)
- [39] F. Fumero et al., "RIM-ONE: An open retinal image database for optic nerve evaluation," in *Intl. Symposium on Computer-Based Medical Systems (CBMS)*, 2011.
- [40] A. Diaz-Pinto, S. Morales, V. Naranjo, T. Köhler, J. M. Mossi, and A. Navea, "Cnns for automatic glaucoma assessment using fundus images: an extensive validation," *Biomedical engineering online*, vol. 18, no. 1, p. 29, 2019.
- [41] Z. Zhang, F. S. Yin, J. Liu, W. K. Wong, N. M. Tan, B. H. Lee, J. Cheng, and T. Y. Wong, "Origa-light: An online retinal fundus image database for glaucoma analysis and research," in *2010 Annual International Conference of the IEEE Engineering in Medicine and Biology. IEEE*, 2010, pp. 3065–3068.
- [42] A. Budai, R. Bock, A. Maier, J. Hornegger, and G. Michelson, "Robust vessel segmentation in fundus images," *International journal of biomedical imaging*, vol. 2013, 2013.
- [43] J. Sivaswamy, A. Chakravarty, G. Datt Joshi, T. Abbas Syed, *JSM Biomedical Imaging Data Papers, A Comprehensive Retinal Image Dataset for the Assessment of Glaucoma from the Optic Nerve Head Analysis*, *JSM Biomed Imaging Data Pap* 2 (1) (2015) 1–7.
- [44] S. Choi, "sjchoi86-HRF Database," github.com/yiweichen04/retina_dataset, Accessed: 09-09-2019.
- [45] P. Porwal, S. Pachade, R. Kamble, M. Kokare, G. Deshmukh, V. Sahasrabudhe, and F. Meriaudeau, "Indian diabetic retinopathy image dataset (IDRID): A database for diabetic retinopathy screening research," *Data*, vol. 3, no. 3, p. 25, Jul. 2018

- [46] Staal, J.J. Abramoff, M.D. Niemeijer, M. Viergever, and M.A. Ginneken, B. 2004. Ridge based vessel segmentation in color images of the retina. *IEEE Transactions on Medical Imaging*, 501-509.
- [47] Messidor-2 Data is Available for Researchers in the Public Domain At. Accessed: Jun. 18, 2019. (Online). Available: <https://medicine.uiowa.edu/eye/abramoff>
- [48] The new MIAS Database. <http://www.wiau.man.ac.uk/services/MIAS/MIASfaq.html>.
- [49] M. Heath et al., "The digital database for screening mammography," in *Proc. of the 5th Int. Workshop on Digital Mammography* 431-434 (2000).
- [50] Sung, J.; Ponce, C.; Selman, B.; Saxena, A. Unstructured human activity detection from rgb-d images. In *Proceedings of the 2012 IEEE International Conference on Robotics and Automation (ICRA)*, St. Paul, MN, USA, 14-18 May 2012; pp. 842-849
- [51] Gasparini, S.; Cipitelli, E.; Gambi, E.; Spinsante, S.; Wähslén, J.; Orhan, I.; Lindh, T. Proposal and experimental evaluation of fall detection solution based on wearable and depth data fusion. In *ICT Innovations 2015*; Springer: Cham (ZG), Switzerland, 2016; pp. 99-108
- [52] Junji Shiraishi, Shigehiko Katsuragawa, Junpei Ikezoe, Tsuneo Matsumoto, Takeshi Kobayashi, Ken-ichi Komatsu, Mitate Matsui, Hiroshi Fujita, Yoshie Kodera, and Kunio Doi. Development of a digital image database for chest radiographs with and without a lung nodule: receiver operating characteristic analysis of radiologists' detection of pulmonary nodules. *American Journal of Roentgenology*, 174(1):71-74, 2000
- [53] Wang X, Peng Y, Lu L, Lu Z, Bagheri M, Summers RM. ChestX-Ray8: Hospital Scale Chest X-Ray Database and Benchmarks on Weakly-Supervised Classification and Localization of Common Thorax Diseases. In: 2017 IEEE Conference on Computer Vision and Pattern Recognition (CVPR), Honolulu, July 21-26, 2017. Piscataway, NJ: IEEE, 2017; 3462-3471.
- [54] Summers RM. NIH Chest X-ray Dataset of 14 Common Thorax Disease Categories. <https://nihcc.app.box.com/v/ChestXray-NIHCC/file/220660789610>. Accessed May 2019.
- [55] <http://challenge2017.isic-archive.com/>
- [56] Amin, J., Sharif, M., Yasmin, M. and Fernandes, S.L., 2020. A distinctive approach in brain tumor detection and classification using MRI. *Pattern Recognition Letters*, 139, pp.118-127.
- [57] Saba, T., Mohamed, A.S., El-Affendi, M., Amin, J. and Sharif, M., 2020. Brain tumor detection using fusion of hand crafted and deep learning features. *Cognitive Systems Research*, 59, pp.221-230.
- [58] Rehman, A., Khan, M.A., Saba, T., Mehmood, Z., Tariq, U. and Ayesha, N., 2021. Microscopic brain tumor detection and classification using 3D CNN and feature selection architecture. *Microscopy Research and Technique*, 84(1), pp.133-149.
- [59] Yu, S., Xiao, D., Frost, S. and Kanagasingam, Y., 2019. Robust optic disc and cup segmentation with deep learning for glaucoma detection. *Computerized Medical Imaging and Graphics*, 74, pp.61-71.
- [60] Serte, S. and Serener, A., 2019, October. A generalized deep learning model for glaucoma detection. In *2019 3rd International symposium on multidisciplinary studies and innovative technologies (ISMSIT)* (pp. 1-5). IEEE.
- [61] Bajwa, M.N., Singh, G.A.P., Neumeier, W., Malik, M.I., Dengel, A. and Ahmed, S., 2020, July. G1020: A Benchmark Retinal Fundus Image Dataset for Computer-Aided Glaucoma Detection. In *2020 International Joint Conference on Neural Networks (IJCNN)* (pp. 1-7). IEEE.
- [62] Pour, A.M., Seyedarabi, H., Jahromi, S.H.A. and Javadzadeh, A., 2020. Automatic detection and monitoring of diabetic retinopathy using efficient convolutional neural networks and contrast limited adaptive histogram equalization. *IEEE Access*, 8, pp.136668-136673.
- [63] Kanjanasurat, I., Purahong, B., Pintavirooj, C., Satayarak, N. and Benjangkaprasert, C., 2020, September. Blood Vessel Extraction and Optic Disk Localization for Diabetic Retinopathy. In *Proceedings of the 2020 10th International Conference on Biomedical Engineering and Technology* (pp. 112-116).
- [64] Arumugam, K., 2021. Chaotic Duck Traveler Optimization (cDTO) Algorithm for Feature Selection in Breast Cancer Dataset Problem. *Turkish Journal of Computer and Mathematics Education (TURCOMAT)*, 12(4), pp.250-262.
- [65] Agarwal, R., Diaz, O., Lladó, X., Yap, M.H. and Martí, R., 2019. Automatic mass detection in mammograms using deep convolutional neural networks. *Journal of Medical Imaging*, 6(3), p.031409.
- [66] Martínez-Villaseñor, L., Ponce, H., Brieva, J., Moya-Albor, E., Núñez-Martínez, J. and Peñafort-Asturiano, C., 2019. UP-fall detection dataset: A multimodal approach. *Sensors*, 19(9), p.1988.
- [67] Gaál, G., Maga, B. and Lukács, A., 2020. Attention u-net based adversarial architectures for chest x-ray lung segmentation. *arXiv preprint arXiv:2003.10304*.
- [68] Majkowska, A., Mittal, S., Steiner, D.F., Reicher, J.J., McKinney, S.M., Duggan, G.E., Eswaran, K., Cameron Chen, P.H., Liu, Y., Kalidindi, S.R. and Ding, A., 2020. Chest radiograph interpretation with deep learning models: assessment with radiologist-adjudicated reference standards and population-adjusted evaluation. *Radiology*, 294(2), pp.421-431.
- [69] Codella, N.C., Gutman, D., Celebi, M.E., Helba, B., Marchetti, M.A., Dusza, S.W., Kalloo, A., Liopyris, K., Mishra, N., Kittler, H. and Halpern, A., 2018, April. Skin lesion analysis toward melanoma detection: A challenge at the 2017 international symposium on biomedical imaging (isbi), hosted by the international skin imaging collaboration (isic). In *2018 IEEE 15th international symposium on biomedical imaging (ISBI 2018)* (pp. 168-172). IEEE.

S. Sowmyayani has done her Ph.D in Computer Science in Manonmaniam Sundaranar University, Tirunelveli, India in 2017. She received her M.Sc Degree in Computer Science from St.Xaviers College(Autonomous), Tirunelveli, India in 2011 and M.Phil in Computer Science in Manonmaniam Sundaranar University, Tirunelveli, India in 2013.

She is working as an Assistant Professor in the Department of Computer Science at St. Mary's College (Autonomous), Thoothukudi, Tamilnadu, India. Her research area includes image processing, video processing and Machine Learning. She has published 2 Indian Patents, international book, book chapter and 14 international articles and 4 international conferences. She is one of the editorial board members in International Journal of Computer Science. She is one of the editorial board members in Edwin Incorporation.